Research Article

Effect of Absorbents on NO$_x$ Removal through Polyvinylidene Fluoride (PVDF) Hollow Fiber Membrane Modules

Irfan Purnawan [iD],[1] **Sutrasno Kartohardjono** [iD],[1] **Levana Wibowo,**[1]
Annisa Faiza Ramadhani,[1] **Woei Jye Lau** [iD],[2] **and Arifina Febriasari** [iD][1]

[1]*Department of Chemical Engineering, Faculty of Engineering, Universitas Indonesia, Kampus UI, Depok 16424, Indonesia*
[2]*Advanced Membrane Technology Research Centre, Universiti Teknologi Malaysia, 81310 Skudai, Johor, Malaysia*

Correspondence should be addressed to Sutrasno Kartohardjono; sutrasno@che.ui.ac.id

NOx (NO and NO$_2$) are air toxins that endanger life and represent a hazard to the environment, such as photochemical smog, global warming, acid rain, ozone depletion, and the occurrence of respiratory infections. Some technological strategies to diminish NOx emissions to meet regulations depend on two techniques: the dry process and the wet process. This study applies polyvinylidene fluoride (PVDF) hollow fiber membrane modules as a medium to remove NOx from solutions containing several absorbents such as hydrogen peroxide and nitric acid (H$_2$O$_2$-HNO$_3$) solutions, sodium chlorite and sodium hydroxide (NaClO$_2$-NaOH) solutions, and sodium chlorate and sodium hydroxide (NaClO$_3$-NaOH) solutions. The experimental results showed that the oxidant's strength influences NOx removal efficiency, where the absorbent solutions containing hydrogen peroxide had the highest removal efficiency as hydrogen peroxide is the most potent oxidant, followed by sodium chlorite and sodium chlorate. The three pairs of absorbents also gave a high NOx removal efficiency (above 90%), which means that all the absorbents used in the study are very potential to be used to diminish NOx via the wet process. NOx removal efficiency at the same feed gas flow rate increased as the number of fiber and absorbent concentrations is increased. However, NOx removal efficiency is reduced as the feed gas flow rate is increased at the same membrane module and absorbent concentration.

1. Introduction

Nitrogen oxides, which are also called NOx (NO and NO2), are generally released from petroleum derivatives, especially in their utilization in power generation and industrial manufacture, hazard life, and threaten the environment [1–5]. Over recent decades, NOx has been viewed as a significant air pollutant, which harms the human body and causes a progression of serious environmental issues, such as photochemical smog, global warming, acid rain, ozone depletion, and the rate of respirational infections [6–12]. Hence, several strategies to lessen NOx emissions have been examined, particularly for diesel and lean-burn gasoline engines whose exhaust fumes contain excess O$_2$ [13–17].

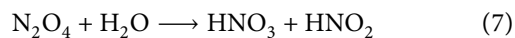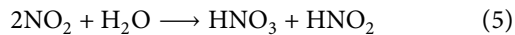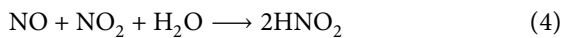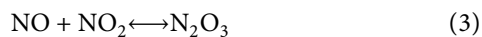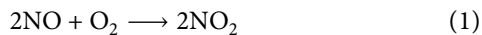A few innovative strategies have been created to lessen NOx emissions to fulfill the guidelines and are fundamentally dependent on two techniques: the dry process and wet process [18]. The dry process incorporates selective catalytic reduction (SCR) [19, 20] and NOx storage and reduction (NSR), which is otherwise called lean-NOx trap (LNT) [21]. SCR employs ammonia as a reducing agent on a catalyst based on vanadium pentoxide-tungsten trioxide/titanium dioxide or copper- and iron-zeolites [22, 23]. Meanwhile, NSR is the most popular lean-NOx reduction technology and the catalysis technology of choice, which is also recognized as LNT or NAC (NOx absorber catalysts) [21].

The wet process gives a few preferences over the dry process, such as adaptation to flue gas, low working temperature, and no catalyst deactivation and degradation over the long run [24]. Nonetheless, NOx removal is still dealing with the issue as insoluble NO possesses an

enormous extent of the gas [25]. One technique is the oxidation of NO to NO_2, which has a lot higher solubility [26]. The wet process utilizes a strong oxidant to convert insoluble NOx species by oxidation into more soluble species. Several strong oxidants solutions include sodium chlorate ($NaClO_3$) [27], sodium chlorite ($NaClO_2$)/sodium hydroxide (NaOH) [28], hydrogen peroxide (H_2O_2)/nitric acid (HNO_3), and potassium permanganate [5]. The wet process utilizes a bubble reactor to remove NOx by the oxidant solutions [27].
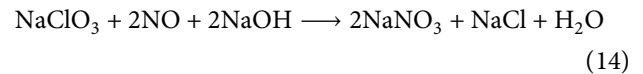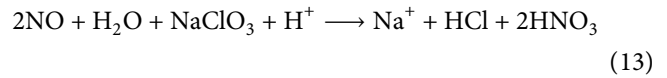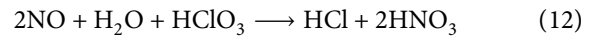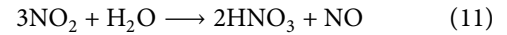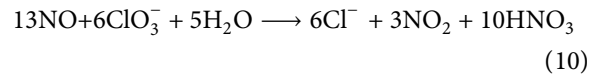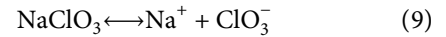
This study applies the PVDF (polyvinylidene fluoride) hollow fiber membrane module as a bubble reactor for NOx absorption into solutions containing several absorbents such as a mixture of nitric acid and hydrogen peroxide solutions, sodium chlorate and sodium hydroxide solutions, and sodium chlorite and sodium hydroxide solutions. PVDF is widely known to have several advantages, such as excellent mechanical strength, high thermal stability, high hydrophobicity, and good chemical resistance [29–31]. In a conventional bubble reactor, bubbles are generated from a feed gas stream containing NOx through the tubing, directly fed into the reactor containing the absorbent solution [27]. In this study, the shell side of the membrane module containing absorbent solutions act as a reactor, and the membrane fibers act to distribute feed gas containing NOx through the membrane pores into the shell side of the membrane module, where the reactions occur between NOx and absorbent solutions. In addition, the hollow fiber membrane module is expected to provide a large contact area between gas and absorbent to enhance the reaction between NOx and absorbent, which leads to an increase in the NOx removal process.

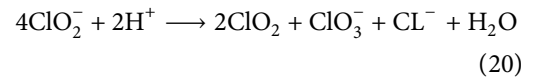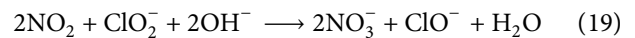The NOx removal reactions through a mixture of H_2O_2 and HNO_3 are as follows [32]:

$$2NO + O_2 \longrightarrow 2NO_2 \tag{1}$$

$$2NO_2 \longleftrightarrow N_2O_4 \tag{2}$$

$$NO + NO_2 \longleftrightarrow N_2O_3 \tag{3}$$

$$NO + NO_2 + H_2O \longrightarrow 2HNO_2 \tag{4}$$

$$2NO_2 + H_2O \longrightarrow HNO_3 + HNO_2 \tag{5}$$

$$N_2O_3 + H_2O \longrightarrow 2HNO_2 \tag{6}$$

$$N_2O_4 + H_2O \longrightarrow HNO_3 + HNO_2 \tag{7}$$

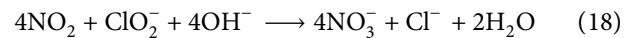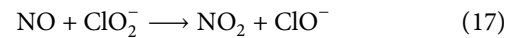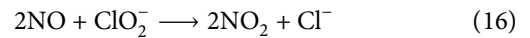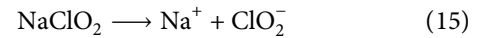$$HNO_2 + H_2O_2 \longrightarrow HNO_3 + H_2O \tag{8}$$

The addition of nitric acid, which acts as an autocatalytic reaction, increases the reaction (8) rate and increases the absorption rate of NOx for trivalent species (HNO_2 and N_2O_3) [33].

The NOx removal reactions through a mixture of $NaClO_3$ and NaOH are as follows [27]:

$$NaClO_3 \longleftrightarrow Na^+ + ClO_3^- \tag{9}$$

$$13NO + 6ClO_3^- + 5H_2O \longrightarrow 6Cl^- + 3NO_2 + 10HNO_3 \tag{10}$$

$$3NO_2 + H_2O \longrightarrow 2HNO_3 + NO \tag{11}$$

$$2NO + H_2O + HClO_3 \longrightarrow HCl + 2HNO_3 \tag{12}$$

$$2NO + H_2O + NaClO_3 + H^+ \longrightarrow Na^+ + HCl + 2HNO_3 \tag{13}$$

$$NaClO_3 + 2NO + 2NaOH \longrightarrow 2NaNO_3 + NaCl + H_2O \tag{14}$$

Meanwhile, the NOx removal reactions through a mixture of $NaClO_2$ and NaOH are as follows [34]:

$$NaClO_2 \longrightarrow Na^+ + ClO_2^- \tag{15}$$

$$2NO + ClO_2^- \longrightarrow 2NO_2 + Cl^- \tag{16}$$

$$NO + ClO_2^- \longrightarrow NO_2 + ClO^- \tag{17}$$

$$4NO_2 + ClO_2^- + 4OH^- \longrightarrow 4NO_3^- + Cl^- + 2H_2O \tag{18}$$

$$2NO_2 + ClO_2^- + 2OH^- \longrightarrow 2NO_3^- + ClO^- + H_2O \tag{19}$$

$$4ClO_2^- + 2H^+ \longrightarrow 2ClO_2 + ClO_3^- + CL^- + H_2O \tag{20}$$

2. Materials and Methods

2.1. PVDF Hollow Fiber Membrane Preparation. The doped solution was prepared by dissolving polymeric pellets insolvent in the presence of an additive. At first, 5 g of PVP K40 was added into 77 g of NMP; both are provided by Sigma Aldrich, Malaysia, under vigorous stirring. After the additive was completely dissolved, 18 g of PVDF pellets (Kynar 760) were slowly added into the mixture to avoid agglomeration. The mixing was continuously stirred overnight to ensure a homogenous solution could be produced. The solution is composed of 18 wt.% PVDF, 5 wt.% PVP K40, and 77 wt% NMP which was then subjected to an ultrasonication process to remove any air bubbles before it could be used for the spinning process.

A self-customized hollow fiber spinning machine was employed to synthesize the hollow fiber membranes using the dope solution prepared. The fabrication process was based on the dry-jet wet spinning method in which an air gap of 5 cm was applied between a spinneret and a water coagulation bath. The hollow fiber membrane was produced using a spinneret with an OD/ID of 1.15 mm/ 0.55 mm. The dope extrusion rate and bore fluid flow rate (pure water) remained at 5 mL/min, respectively, throughout the process. The as-spun fiber was then

collected using a wind-up drum at a speed of 10 m/min. After that, the fiber was immersed 24 h in a pure water bath to remove any solvent before being posttreated with 10 wt.% glycerol solution. Finally, it was air-dried at room conditions. FESEM and FEI inspected F50 was used to investigate the membrane morphology.

2.2. NOx Removal Experiment. The experimental scheme for the NOx removal process through the hollow fiber membrane module is shown in Figure 1. The membrane module contains 40, 50, and 59 PVDF-based fibers with sizes of 0.5 mm, 1.5 mm, and 40 cm in diameter, outer diameter, and length, respectively. The chemicals used, such as H_2O_2, $NaClO_2$, $NaClO_3$, HNO_3, and $NaOH$, are analytical grade bought from Merck, Indonesia. Meanwhile, the feed gas, provided by Energi Indogas Nusantara, Indonesia, utilized contains around 600 ppm NOx in the air. The flow rate of the NOx-containing gas to the membrane module through the fiber's lumen is regulated by the mass flow controller, CX Series, Shanghai Instrument. For the experiment purpose, one end of the tube and shell sides of the membrane module is closed so that in the tubing section, only have one input for the feed gas stream and, in the shell side of the membrane module, one output serves the gas outlet is present. Prior to the NOx removal experiment, the absorbent liquid was first introduced into the shell side of the hollow fiber membrane module. During the experiment, the feed gas enters the lumen fibers and then diffuses through the membrane pores and exits the fiber to the shell side of the membrane module, where the reaction occurs between NOx and the absorbent solutions. Finally, the lean-NOx gas concentration exited from the membrane module is measured using the Ecom-D Gas Analyzer. The observed parameters of the experiments are the NOx removal efficiency, %R, the overall mass transfer coefficient, K_G, flux, J, absorbed NOx, and the NOx loading, and they are calculated as follows [5, 35, 36]:

$$\%R = 100 \frac{C_{\text{in}} - C_{\text{out}}}{C_{\text{in}}}, \tag{21}$$

$$J = \frac{NOx_{\text{Abs}}}{A_m}, \tag{22}$$

$$NO_{x-\text{loading}} = \frac{NOx_{\text{abs}}}{\text{mole oxidant}}, \tag{23}$$

$$NOx_{\text{abs}} = (C_{\text{in}} - C_{\text{out}})Q_G \frac{P}{RT}. \tag{24}$$

C_{in} and C_{out} are NOx concentrations in the feed gas and lean-NOx exit from the membrane module, respectively; Q_G, A_m, and NOx_{abs} are the feed gas flow rate, fiber surface area, and mole NOx absorbed by the absorbents, respectively. The mole oxidant is the number of moles of H_2O_2, $NaClO_2$, or $NaClO_3$ in absorbent solutions. Meanwhile, P, R, and T are the pressure, ideal gas constant, and temperature, respectively.
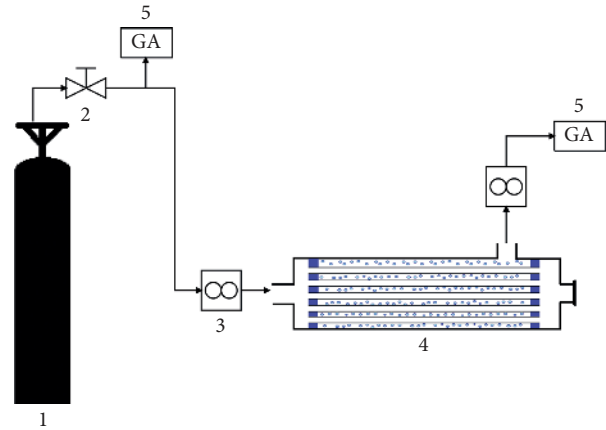

Figure 1: Schematic diagram of NOx removal experiment: 1. feed gas tank; 2. valve regulator; 3. mass flow controller; 4. hollow fiber membrane module; 5. gas analyzer.

3. Results and Discussion

3.1. Membrane Morphology. The SEM analysis results in Figure 2 indicate that the hollow fiber membrane structure is asymmetric [37, 38]. In the cross section, it can be seen that the outer surface of the membrane looks denser, while the inside of the membrane shows a layer of macro voids that was formed with a sponge-like structure. The top surface image also confirmed the asymmetric structure, where the pore size appears nonuniform. The smaller pore sizes were distributed and appeared at a magnification of 10000 times, while some of the larger pores were nonuniformly distributed. Based on the porosity measurements, the membrane porosity was obtained at 71.04 ± 6.04 and the thickness around $115\,\mu$m. The porosity value is in line with the SEM results obtained, where the pores of the membrane appear to be well distributed even though the pore size is nonuniform [39].

3.2. Effect of Feed Gas Flow Rate. To see the impact of the feed gas flow rate on the NOx removal efficiency and the NOx absorbed, the NOx removal experiment were conducted using volume and concentration of the H_2O_2-HNO_3, $NaClO_2$-$NaOH$, and $NaClO_3$-$NaOH$ absorbent pairs 200 ml/200 ml and 0.1 M/0.5 M, respectively. Meanwhile, the flow rate of the feed gas was varied from 0.1 to 0.2 L/min in a membrane module containing 40 fibers. The feed gas entered the lumen fiber and then passed through the fiber toward the membrane module's shell side, causing bubbles to appear. The bubbles generated by the feed gas in the membrane module are shown in Figure 3. The NOx removal process occurs due to its reaction with the absorbents, as in equations (1)–(20), in the gas–liquid interface on the outside of the fibers, and the bulk of absorbent solutions in the membrane module [5].

As demonstrated in Figure 4, the NOx removal efficiency declines as the feed gas flow rate into the membrane module increases. The amount of NOx that can be absorbed, as shown in Figure 4, increases with the feed gas flow rate, and

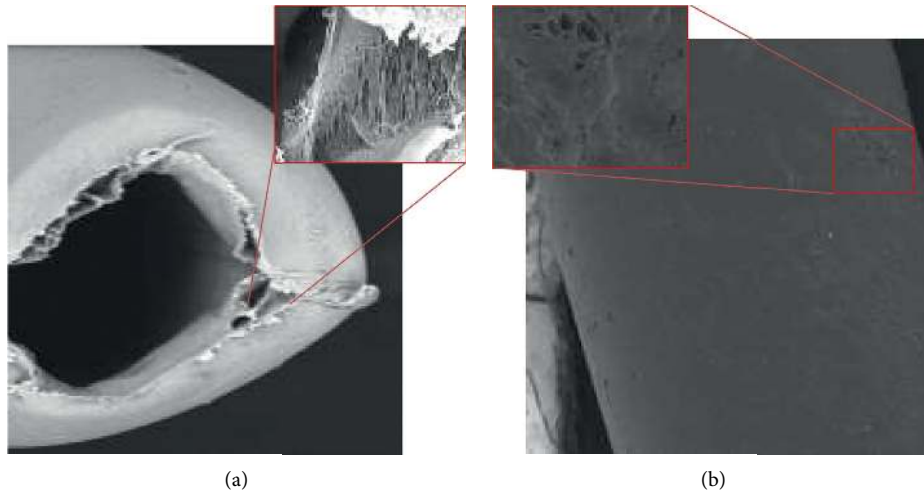(a)   (b)

FIGURE 2: SEM micrograph of (a) cross section and (b) top surface of PVDF hollow fiber membrane.

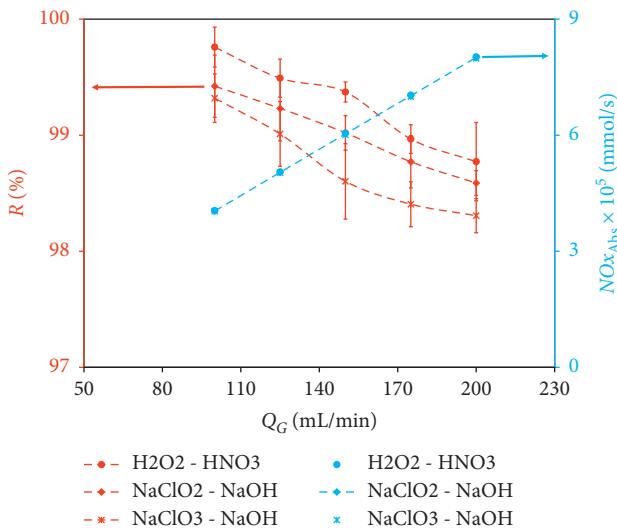FIGURE 3: Bubbles appeared during the NOx removal experiment.

FIGURE 4: The feed gas flow rate, Q_G, effects on the NOx removal efficiency, R, and the amount of NOx absorbed $NOxAbs$ in a 40 fiber membrane module using 400 mL of absorbent pairs of H_2O_2 (0.05 M) - HNO_3 (0.25 M), $NaClO_2$ (0.05 M) – NaOH (0.25 M), and $NaClO_3$ (0.05 M) – NaOH (0.25 M).

based on equation (21), it increases the removal efficiency. However, based on equation (21), increasing the feed gas flow rate can reduce NOx removal efficiency. The decrease in

NOx removal efficiency indicates that the feed gas flow rate increment is superior to the absorbed NOx. In other words, the residence time of the gas in the membrane module decreases as the feed gas flow rate is increased, which leads to decreasing the contact time between the NOx and the absorbents, and finally reduces NOx removal efficiency [5]. Figure 4 also shows that all adsorbent solutions used have a higher efficiency than 90%, which indicates that all adsorbent solutions used have a good ability to remove NOx from the feed gas stream. The NOx removal efficiency for the absorbent pairs of H_2O_2/HNO_3, $NaClO_2/NaOH$, and $NaClO_3/NaOH$ was slightly decreased from 99.8 to 98.8%, 99.4 to 98.6%, and 99.3 to 98.3%, or decreased by approximately 1.00, 0.80 and 1.01%, respectively, when the feed gas flow rate, containing 600 ppm of NOx, increase from 0.1 to 0.2 L/min. Absorbent containing H_2O_2 has the highest efficiency because it has the highest oxidizing strength, followed by $NaClO_2$ and $NaClO_3$. The potential reduction standards of H_2O_2, $NaClO_2$, and $NaClO_3$ are 1.77, 0.76, and 0.62 V, respectively [40]. Meanwhile, the increase in the NOx absorbed by the three pairs of absorbents was almost the same, from about 4.0×10^{-5} to 7.9×10^{-5} mmol/s as the three pairs' removal efficiency only differed slightly. Similar results were shown in previous studies where the NOx removal efficiency slightly decreased from 99.6% to 98.9% or decreased by 0.7% when the feed gas flow rate increased from 0.1 to 0.2 L/min on a polysulfone hollow fiber membrane module having a mixture of 75 mL 0.5 wt.% of H_2O_2 and 75 mL 0.5 M of HNO_3, and the amount of fiber 100. Wang and Yu also reported a decrease in NOx removal efficiency in a polypropylene membrane module using an absorbent solution containing 5 wt.% and 0.2 wt.% of NaCl and H_2O_2, and a concentration of NO in the feed gas of about 185 ppm, where the NO removal efficiency decreased from 91% to 29% as the feed gas flow rate increased from 0.05 to 0.25 L/min [41].

Figure 5(a) presents that the flux, J, increases with the feed gas flow rate in a membrane module containing 40 fibers. The thickness of the gas-liquid boundary layer
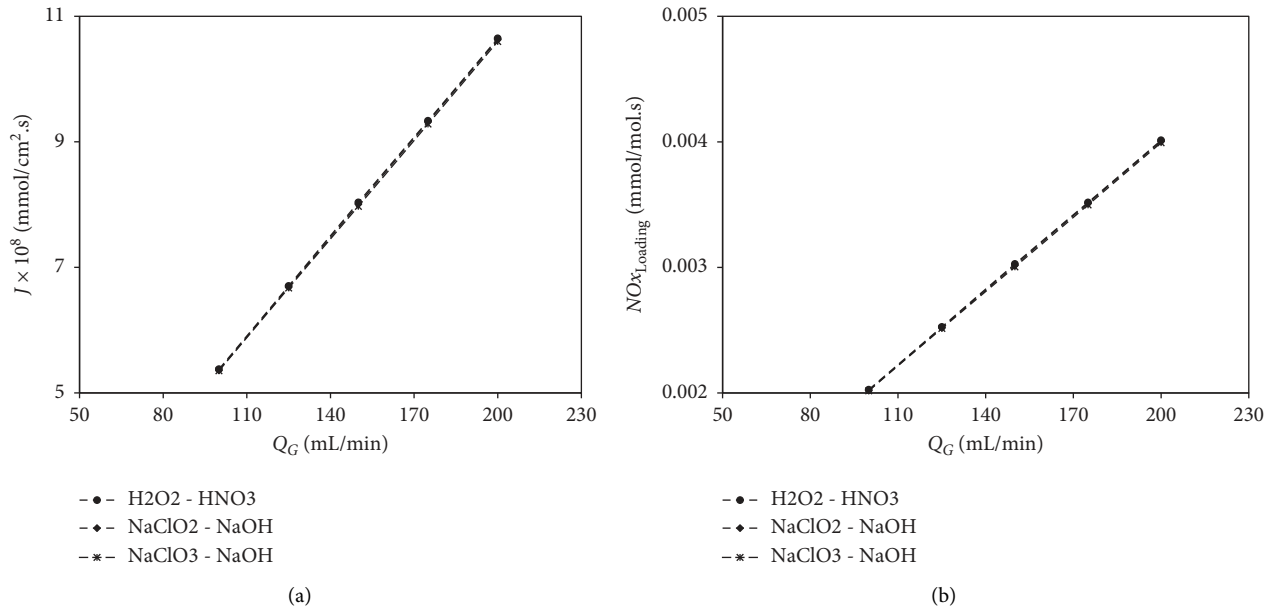
FIGURE 5: Effect of feed gas flow rate, Q_G, on (a) the flux, J; (b) the NOx loading in a membrane module containing 40 fibers using 400 mL of absorbent pairs of H_2O_2 (0.05 M) - HNO_3 (0.25 M), $NaClO_2$ (0.05 M) – NaOH (0.25 M), and $NaClO_3$ (0.05 M) – NaOH (0.25 M).

decreases with the feed gas flow rate increment, thereby increasing the NOx transfer driving force, the gas diffusion rate, and the absorbed NOx [42]. Furthermore, according to equations (22)–(24), the flux increase as the absorbed NOx is increased in the same membrane surface area. The flux for the three pairs of absorbents was relatively the same as the amount of NOx absorbed for the three pairs of absorbents only differed slightly. The three pairs of absorbents had almost the same increase in flux from about 5.4×10^{-8} to 1.1×10^{-7} mmol/cm^2.s as the feed gas flow rate is doubled from 0.1 to 0.2 L/min. Previous studies have also shown similar results where the absorbed NOx flux increases from about 0.0026 to 0.0051 mol/m^2.h as the feed gas flow rate, containing 600 ppm NOx, is increased from 0.1 to 0.2 L/min in a membrane module containing 32 polysulfone-based fibers and a mixture of 0.5 wt.% H_2O_2 and 0.5 M HNO_3 each of 25 mL as an absorbent solution [5].

NOx loading, the ratio between the rate of moles of NOx absorbed (mmol/s) and the moles of oxidants used (H_2O_2, $NaClO_2$, and $NaClO_3$) in the absorbent solution, is shown in Figure 5(b). As with the absorbed NOx, the NOx loading for the three absorbent pairs (H_2O_2-HNO_3, $NaClO_2$-NaOH, and $NaClO_3$-NaOH) increased as the feed gas flow rate was increased, and had almost the same value due to the same moles of oxidants in the absorbent solutions. As demonstrated in Figure 5(b), the NOx loading increases linearly from about 0.002 to 0.004 mmol/mol.s with increasing the feed gas flow rate from 0.1 to 0.2 L/min due to increasing NOx absorbed.

3.3. Effect of the Number of Fibers in the Membrane Module. The increase in the number of fibers in the membrane module increases the gas-liquid contact surface area, and bubbles are formed. These two factors enhance the mass

transfer process to increase the amount of NOx absorbed, which leads to an increase in NOx removal efficiency and NOx loading because it uses the same feed gas flow rate and absorbent concentration, as shown in Figure 6(a). The absorbent pair containing H_2O_2-HNO_3 gave the highest removal efficiency and NOx loading compared to the other two absorbent pairs ($NaClO_2$-NaOH and $NaClO_3$-NaOH) due to the strongest oxidation properties compared to the other two oxidants [37]. On the other hand, the flux and mass transfer coefficient decrease with the number of fibers in the membrane module, as presented in Figure 6(b). The fiber number increment in the membrane module certainly increases the absorbed NOx and enhances the mass transfer process. However, the fiber number increment leads to an increase in the membrane's gas-liquid contact and reduces the mass transfer performance as expressed in equation (24) [42]. The mass transfer coefficient of the H_2O_2-HNO_3 absorbent pair has the highest value compared to the other two pairs ($NaClO_2$-NaOH and $NaClO_3$-NaOH) due to the strongest oxidation properties [40]. In comparison, the flux for the three pairs of absorbents was relatively the same as the amount of NOx absorbed for the three pairs of absorbents only differed slightly. In this study, the NOx removal efficiency slightly increased from about 99.5 to 99.8%, 99.2 to 99.6%, and 99.0 to 99.3%, or increased by approximately 0.63%, 0.39%, and 0.30% for the absorbent pairs of H_2O_2-HNO_3, $NaClO_2$-NaOH, and $NaClO_3$-NaOH, respectively, with the increment of fiber number in the membrane module from 40 to 59, at 0.125 L/min feed gas rate. A similar result was also reported in previous studies that the NOx removal efficiency increased from about 86 to 97% with the increment of fiber number from 50 to 150, at 0.2 L/min feed gas rate containing 560 ppm of NOx using a mixture of 0.5 wt.% H_2O_2 and 0.5 M HNO_3 each of 75 mL as an absorbent
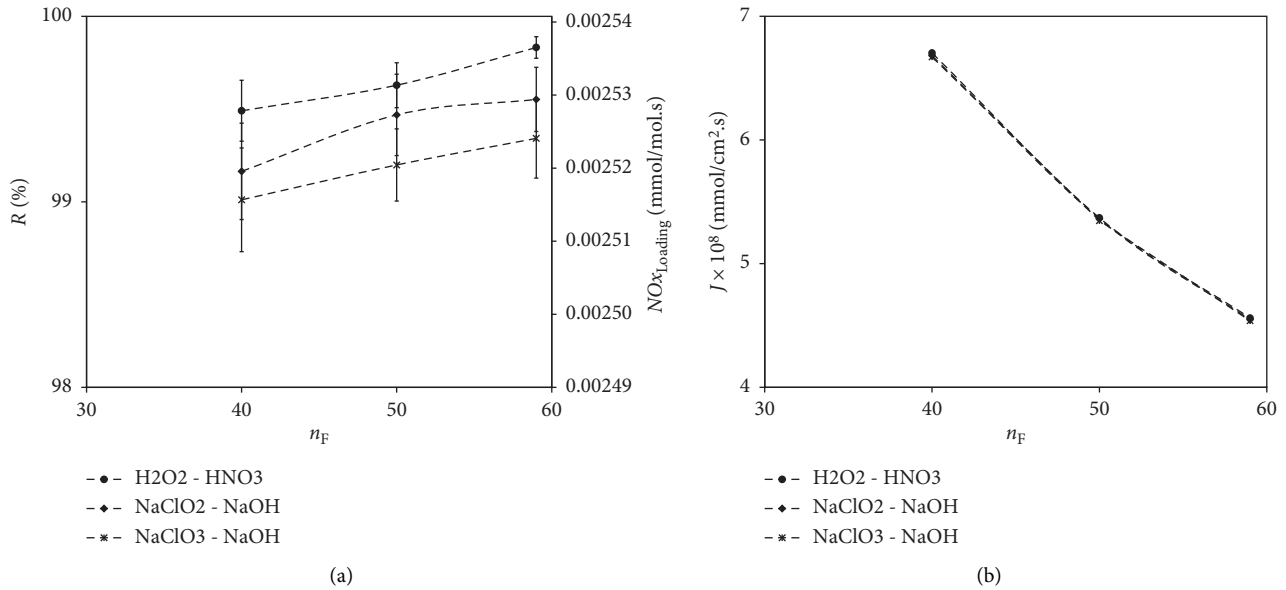
(a)

(b)

FIGURE 6: The effect of the fiber number in the membrane module, n_F, on (a) the NOx expulsion efficiency, R, and NOx loading; (b) the overall mass transfer coefficient, K_G, and flux, J, in a membrane module having 400 mL of absorbent pairs of H_2O_2 (0.05 M) - HNO_3 (0.25 M), $NaClO_2$ (0.05 M) – NaOH (0.25 M), and $NaClO_3$ (0.05 M) – NaOH (0.25 M) at 125 mL/min feed gas rate.
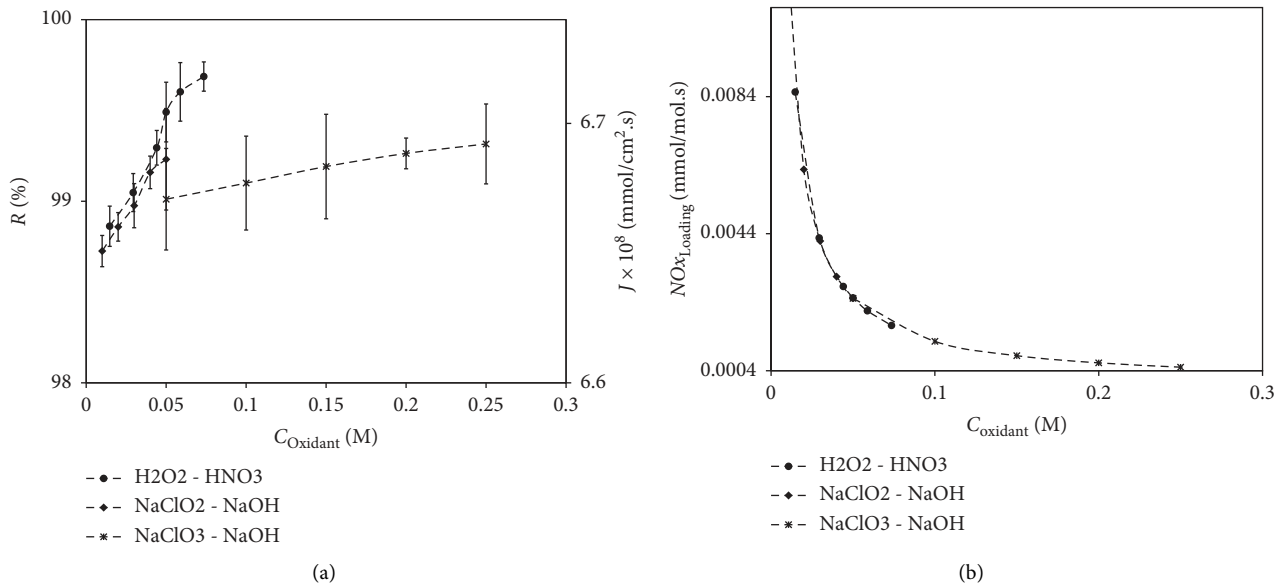

(a)

(b)

FIGURE 7: The fiber in the membrane module, n_F, on (a) the NOx expulsion efficiency, R, and the flux, J; (b) the NOx loading in a membrane module containing 400 mL of absorbent pairs of H_2O_2 (0.05 M) - HNO_3 (0.25 M), $NaClO_2$ (0.05 M) – NaOH (0.25 M), and $NaClO_3$ (0.05 M) – NaOH (0.25 M) at the feed gas flow rate of 125 mL/min.

solution [5]. Another study also reported that NOx absorption efficiency slightly increased by approximately 0.4% from 94.2% to 94.6% with the increment of fiber number in the polysulfone membrane module from 16 to 48, using the absorbent consisting of HNO_3 0.5 M and H_2O_2 0.5% w/t at 1 : 1, and at 0.1 L/min feed gas rate [42].

The flux for the three absorbent pairs in this study decreased from about 6.7 to 4.5×10^{-8} mmol/cm². s or

approximately 32% decreased with the increment of fiber number in the membrane module from 40 to 59 at 0.125 L/min feed gas rate. The flux decreased was similar to the previous study where the NOx transfer flux declined from 0.0030 to 0.0011 mol/m².h or 62% reduced with the fiber number increment in the polysulfone membrane module from 50 to 150, at 0.2 L/min feed gas rate applying a mixture of 0.5 wt.% H_2O_2 and 0.5 M HNO_3 each of 75 ml as absorbents [5].

3.4. Effect of the Oxidant Concentration. The increase in the oxidant concentration (H_2O_2, $NaClO_2$, or $NaClO_3$) increases the number of moles of oxidants, as expressed in equations (2), (8), and (14) in the absorbent solution, which, in turn, enhances the mass transfer process to increase the amount of NOx absorbed. It leads to an increase in the NOx removal efficiency and flux, as presented in Figure 7(a), due to the same feed gas rate and the membrane module used in the experiment. On the other hand, an increase in oxidant concentration (H_2O_2, $NaClO_2$, or $NaClO_3$) reduces NOx loading because the increase in the amount of NOx absorbed is not proportional to the increase in the concentration of oxidant. According to equation (23), increasing the concentration of oxidant is more dominant than the increase in NOx absorbed, which causes a decrease in NOx loading. The NOx removal efficiency for absorbents containing H_2O_2, $NaClO_2$, and $NaClO_3$ oxidants increased from 98.9 to 99.7%, 98.7 to 99.2%, and 99.0 to 99.3% when the oxidant concentration increased from 0.015 to 0.075 M, 0.01 to 0.05 M, and 0.05 to 0.25 M, respectively, in a 40 fibers membrane module and the flow rate of the feed gas of around 0.125 L/min. The absorbent volume in the membrane module is 400 mL consisting of 200 ml of the oxidant and 200 ml of 0.5 M HNO_3 for H_2O_2 or 0.5 M $NaOH$ for $NaClO_3$.

Meanwhile, for the same operating conditions, NOx loading decreased because the increase in the amount of NOx absorbed is not proportional to the increase in oxidants' concentration in the absorbent solution, as presented in Figure 7(b). Figure 7(b) also shows that the three pairs of absorbents have almost the same NOx loading because the amount of NOx absorbed by the three absorbents is also only slightly different. Previous studies gave similar results where the NOx removal efficiency increased from 93% to 95% with an increase in the concentration of H_2O_2 from 0.25 to 2.5 wt.% in the absorbent solution containing H_2O_2 and 0.5 M HNO_3 each of 25 mL in a 32 fiber polysulfone membrane module and the flow rate of the feed gas of around 0.15 L/min [5]. A similar result was also reported by Shi et al. [27] using a bubble column reactor where an increase in the concentration of $NaClO_3$ from 0.005 M to 0.1 M led to an increase in NOx removal efficiency from 35.48% to 91.65%.

4. Conclusion

The three pairs of absorbents, H_2O_2-HNO_3, $NaClO_2$-$NaOH$, and $NaClO_3$-$NaOH$, provided a high NOx removal efficiency (above 90%), which indicated that all the absorbents applied in the study are very potential to be used for NOx removal in the wet process. The hollow fiber membrane module could be utilized as the bubble reactor to diminish NOx from the gas stream using three pairs of absorbents. The oxidant's strength affects the NOx removal efficiency, where the absorbent containing H_2O_2 provided the best removal efficiency because of its most potent oxidation properties compared to $NaClO_2$ and $NaClO_3$. The experiments also showed that the NOx removal efficiency increased with the fiber number in the membrane module and absorbent concentration. However, the NOx removal efficiency decreased with the feed gas flow rate. In the actual condition, the flue gas from fossil fuel combustion contains not only NOx but also SO_2. Therefore, a future study is also necessary to reduce both NOx and SO_2 simultaneously in the membrane module, which functions as a bubble reactor.

Data Availability

The data used to support the findings of this study are available from the corresponding author upon request.

Conflicts of Interest

The authors declare that they have no conflicts of interest.

Acknowledgments

References

[1] Y. Liu, Q. Wang, and J. Pan, "Novel process of simultaneous removal of nitric oxide and sulfur dioxide using a vacuum ultraviolet (VUV)-activated O_2/H_2O/H_2O_2 system in a wet VUV–spraying reactor," *Environmental Science and Technology*, vol. 50, no. 23, pp. 12966–12975, 2016.

[2] Y. Zhao, Y. Han, and C. Chen, "Simultaneous Removal of SO_2 and NO from flue gas using multicomposite active absorbent," *Industrial & Engineering Chemistry Research*, vol. 51, no. 1, pp. 480–486, 2012.

[3] J. Ding, Q. Zhong, and S. Zhang, "Simultaneous desulfurization and denitrification of flue gas by catalytic ozonation over Ce-Ti catalyst," *Fuel Processing Technology*, vol. 128, pp. 449–455, 2014.

[4] J. Ding, Q. Zhong, and S. Zhang, "Catalytic efficiency of iron oxides in decomposition of H_2O_2 for simultaneous NOx and SO_2 removal: effect of calcination temperature," *Journal of Molecular Catalysis A: Chemical*, vol. 393, pp. 222–231, 2014.

[5] S. Kartohardjono, C. Merry, M. S. Rizky, and C. C. Pratita, "Nitrogen oxide reduction through absorbent solutions containing nitric acid and hydrogen peroxide in hollow fiber membrane modules," *Heliyon*, vol. 5, no. 12, Article ID e02987, 2019.

[6] J. Choi, K. S. Lee, D. Y. Choi, Y. J. Kim, and S. S. Kim, "Dry de-NOx process via gas-phase photochemical oxidation using an ultraviolet and aerosolized H_2O/H_2O_2 hybrid system," *Energy & Fuels*, vol. 28, no. 8, pp. 5270–5276, 2014.

[7] L. Gao, C. Li, P. Lu et al., "Simultaneous removal of Hg0 and NO from simulated flue gas over columnar activated coke granules loaded with La_2O_3-CeO_2 at low temperature," *Fuel*, vol. 215, pp. 30–39, 2018.

[8] P. Sun, X. Cheng, Z. Wang, Y. Lai, C. Ma, and J. Chang, "NOx reduction by CO over ASC catalysts in a simulated rotary reactor: effect of reaction conditions," *Journal of the Energy Institute*, vol. 92, no. 3, pp. 488–501, 2019.

[9] J. Zhao, Y. Song, W.-H. Lam et al., "Solar radiation transfer and performance analysis of an optimum photovoltaic/thermal system," *Energy Conversion and Management*, vol. 52, no. 2, pp. 1343–1353, 2011.

[10] R.-t. Guo, W.-g. Pan, X.-b. Zhang et al., "The absorption kinetics of NO into weakly acidic NaClO solution," *Separation Science and Technology*, vol. 48, no. 18, pp. 2871–2875, 2013.

[11] S. Andreoli, F. A. Deorsola, C. Galletti, and R. Pirone, "Nanostructured MnOx catalysts for low-temperature NOx SCR," *Chemical Engineering Journal*, vol. 278, pp. 174–182, 2015.

[12] Z. Liu, J. Hao, L. Fu, and T. Zhu, "Study of Ag/La0 6Ce0 4CoO_3 catalysts for direct decomposition and reduction of nitrogen oxides with propene in the presence of oxygen," *Applied Catalysis B: Environmental*, vol. 44, no. 4, pp. 355–370, 2003.

[13] Z. Liu, J. Li, and S. I. Woo, "Recent advances in the selective catalytic reduction of NOx by hydrogen in the presence of oxygen," *Energy & Environmental Science*, vol. 5, no. 10, pp. 8799–8814, 2012.

[14] X. Huang, J. Ding, and Q. Zhong, "Catalytic decomposition of H_2O_2 over Fe-based catalysts for simultaneous removal of NOx and SO_2," *Applied Surface Science*, vol. 326, pp. 66–72, 2015.

[15] Y. K. Kwon and D. H. Han, "Microwave effect in the simultaneous removal of NOx and SO_2 under electron beam irradiation and kinetic investigation of NOx removal rate," *Industrial & Engineering Chemistry Research*, vol. 49, no. 17, pp. 8147–8156, 2010.

[16] G. Hu, Z. Sun, and H. Gao, "Novel process of simultaneous removal of SO_2 and NO_2 by sodium humate solution," *Environmental Science and Technology*, vol. 44, no. 17, pp. 6712–6717, 2010.

[17] G. Chen, J. Gao, J. Gao et al., "Simultaneous removal of SO_2 and NOx by calcium hydroxide at low temperature: effect of SO_2 absorption on NO_2 removal," *Industrial & Engineering Chemistry Research*, vol. 49, no. 23, pp. 12140–12147, 2010.

[18] O. Ghriss, H. Ben Amor, M.-R. Jeday, and D. Thomas, "Nitrogen oxides absorption into aqueous nitric acid solutions containing hydrogen peroxide tested using a cables-bundle contactor," *Atmospheric Pollution Research*, vol. 10, no. 1, pp. 180–186, 2019.

[19] S. Brandenberger, O. Kröcher, A. Tissler, and R. Althoff, "The state of the art in selective catalytic reduction of NOx by ammonia using metal-exchanged zeolite catalysts," *Catalysis Reviews*, vol. 50, no. 4, pp. 492–531, 2008.

[20] K. Jug, T. Homann, and T. Bredow, "Reaction mechanism of the selective catalytic reduction of NO with NH_3 and O_2 to N_2," *The Journal of Physical Chemistry A*, vol. 108, no. 15, pp. 2966–2971, 2004.

[21] S. Roy and A. Baiker, "NOx storage-reduction catalysis: from mechanism and materials properties to storage-reduction performance," *Chemical Reviews*, vol. 109, no. 9, pp. 4054–4091, 2009.

[22] M. Mehring, M. Elsener, and O. Kröcher, "Selective catalytic reduction of NOx with ammonia over soot," *ACS Catalysis*, vol. 2, no. 7, pp. 1507–1518, 2012.

[23] A. Grossale, I. Nova, and E. Tronconi, "Study of a Fe–zeolite-based system as NH_3-SCR catalyst for diesel exhaust after-treatment," *Catalysis Today*, vol. 136, no. 1-2, pp. 18–27, 2008.

[24] L. Guo, Y. Shu, and J. Gao, "Present and future development of flue gas control technology of DeNO_X in the world," *Energy Procedia*, vol. 17, pp. 397–403, 2012.

[25] F. Yuan, J. Yan, W. Yu, J. Du, and J. Yu, "Nitric oxide reduction by hydrogen peroxide absorption through a ceramic hollow fiber membrane contactor," *Journal of Environmental Chemical Engineering*, vol. 8, no. 5, Article ID 104129, 2020.

[26] R. Hao, Y. Mao, X. Mao et al., "Cooperative removal of SO_2 and NO by using a method of UV-heat/H_2O_2 oxidation combined with NH_4OH-$(NH4)_2SO_3$ dual-area absorption," *Chemical Engineering Journal*, vol. 365, pp. 282–290, 2019.

[27] D. Shi, G. Sun, and Y. Cui, "Study on the removal of NO from flue gas by wet scrubbing using $NaClO_3$," *Journal of the Serbian Chemical Society*, vol. 84, p. 53, 2019.

[28] J.-C. Wei, P. Yu, B. Cai, Y.-B. Luo, and H.-Z. Tan, "Absorption of NO in aqueous $NaClO_2$/Na_2CO_3 solutions," *Chemical Engineering & Technology*, vol. 32, no. 1, pp. 114–119, 2009.

[29] P. Saxena and P. Shukla, "A comprehensive review on fundamental properties and applications of poly (vinylidene fluoride) (PVDF)," *Advanced Composites and Hybrid Materials*, vol. 4, pp. 8–26, 2021.

[30] W. Wang, X. Xu, Z. Zhang, P. Zhang, Y. Shi, and P. Ding, "Study on the improvement of PVDF flat ultrafiltration membrane with MWCNTs-OH as the additive and the influence of different MWCNTs-OH scales," *Colloid and Interface Science Communications*, vol. 43, Article ID 100433, 2021.

[31] X. Tan and D. Rodrigue, "A review on porous polymeric membrane preparation. Part I: production techniques with polysulfone and poly (vinylidene fluoride)," *Polymers*, vol. 11, no. 7, Article ID 1160, 2019.

[32] D. Thomas and J. Vanderschuren, "Analysis and prediction of the liquid phase composition for the absorption of nitrogen oxides into aqueous solutions," *Separation and Purification Technology*, vol. 18, no. 1, pp. 37–45, 1999.

[33] D. Thomas and J. Vanderschuren, "The absorption-oxidation of NOx with hydrogen peroxide for the treatment of tail gases," *Chemical engineering science*, vol. 51, no. 11, pp. 2649–2654, 1996.

[34] T. W. Chien, H. Chu, and H. T. Hsueh, "Kinetic study on absorption of SO_2 and NOx with acidic $NaClO_2$ solutions using the spraying column," *Journal of Environmental engineering*, vol. 129, no. 11, pp. 967–974, 2003.

[35] D. Wang, W. Teo, and K. Li, "Selective removal of trace H2S from gas streams containing CO_2 using hollow fibre membrane modules/contractors," *Separation and Purification Technology*, vol. 35, no. 2, pp. 125–131, 2004.

[36] J. Wang, H. Zhao, G. Haller, and Y. Li, "Recent advances in the selective catalytic reduction of NOx with NH_3 on Cu-Chabazite catalysts," *Applied Catalysis B: Environmental*, vol. 202, pp. 346–354, 2017.

[37] D. Wang, K. Li, and W. Teo, "Porous PVDF asymmetric hollow fiber membranes prepared with the use of small molecular additives," *Journal of Membrane Science*, vol. 178, no. 1-2, pp. 13–23, 2000.

[38] C. Y. Pan, "Gas separation by high-flux, asymmetric hollow-fiber membrane," *AIChE Journal*, vol. 32, no. 12, pp. 2020–2027, 1986.

[39] S. Jamalpour, M. Ghahramani, S. R. Ghaffarian, and M. Javanbakht, "The effect of poly(hydroxyl ethyl methacrylate) on the performance of PVDF/P(MMA-co-HEMA) hybrid gel polymer electrolytes for lithium ion battery application," *Polymer*, vol. 195, Article ID 122427, 2020.

[40] D. R. Lide, *CRC Handbook of Chemistry and Physics*, CRC Press, Boca Raton, FL, USA, 2004.

[41] Y. Wang and X. Yu, "Removal of NO research in a polypropylene hollow fiber membrane contactor," in *Proceedings of the 2017 6th International Conference on Energy, Environment and Sustainable Development (ICEESD 2017)*, Atlantis Press, Paris, France, March 2017.

[42] S. Kartohardjono, M. S. Rizky, E. F. Karamah, and W.-J. Lau, "The effect of the number of fibers in hollow fiber membrane modules for NOx absorption," *Chemical Engineering*, vol. 11, no. 2, pp. 269–277, 2020.